

A Test for the Gluon Selfcoupling in the Reactions $e^+ e^- \rightarrow 4$ Jets and $Z^0 \rightarrow 4$ Jets

O. Nachtmann

Institut für Theoretische Physik der Universität, D-6900 Heidelberg¹ and DESY, D-2000 Hamburg, Federal Republic of Germany

A. Reiter

Institut für Theoretische Physik der Universität, D-6900 Heidelberg, Federal Republic of Germany

Received 22 June 1982

Abstract. We consider the reactions $e^+ e^- \rightarrow \gamma^* \rightarrow 4$ jets and $Z^0 \rightarrow 4$ jets with the 4 jets coming in two pairs of essentially back to back jets of high and low energy. We calculate the angular distribution of the low energy jet axis with respect to the high energy jet axis in QCD, in an abelian gluon model “QED” and a phase space model (PS). Using simple helicity arguments we show that our angular distribution is very sensitive to the triple gluon coupling in QCD. This is then confirmed by a complete calculation. Our correlation offers, therefore, a direct test for QCD as a non-abelian gauge theory.

1) Introduction

Quantumchromodynamics (QCD) is widely believed to be the correct field theory of strong interactions. But to date some important features of this theory remain untested experimentally. Consider the basic particles of QCD: quarks and gluons. Have all their properties, i.e. their quantum numbers and couplings, been established by experiments? Even if quarks and gluons are not known as free particles, all the basic properties of the *quarks* are well established. We have good experimental evidence for their spin, flavour and color charges. Let us remember just one example. At c.m. energies $\sqrt{s} \gtrsim 7$ GeV a two-jet behaviour is observed in $e^+ e^-$ -annihilation into hadrons [1, 2]. This is interpreted as production of a quark–antiquark pair which fragments into hadrons. Information on the spin of the quarks is contained in the angular distribution of the jet axis with respect to the $e^+ e^-$ -beam axis. The observation of a $(1 + \cos^2 \theta)$ behaviour for this jet axis is clear and convincing evidence that quarks have spin 1/2. Also the coupling of quarks to gluons can be considered as established, for instance by the observa-

tion and detailed analysis of 3-jet events in $e^+ e^-$ -annihilation in the continuum [3].

The basic properties of gluons are much less well tested experimentally. There is evidence that gluons have spin 1 from scaling violations in deep inelastic scattering (for a recent experimental analysis cf. e.g. [4], for a review cf. [5]), from Y -decays [6] and from three-jet events in $e^+ e^-$ -annihilation in the continuum [3, 7]. The fact that the Y -particle does not decay predominantly into two jets can be taken as evidence that the gluons carry some internal quantum number like color [8]. If they carry color, gluons must act as their own source in QCD, they must have a selfcoupling. To lowest order this is represented by the triple gluon vertex. Great theoretical effort has been devoted to devise tests for the existence of the triple gluon vertex which is characteristic for the non-abelian nature of QCD. Such tests have been proposed for heavy quarkonium decays [9], for hadron–hadron reactions giving high p_T particles [10], for lepton–nucleon scattering [11] and for $e^+ e^-$ -annihilation into hadrons [12, 13]. Many of the proposed tests involve rather difficult experiments. In any case, such an important feature of QCD as the triple gluon vertex should be tested in a variety of independent reactions.

In this paper we propose a new test for the triple gluon vertex in the following reactions: electron–positron annihilation into four hadron jets via a virtual photon γ^* and Z^0 -boson decay into 4 jets.

$$e^+ + e^- \rightarrow \gamma^* \rightarrow 4 \text{ jets} \quad (1.1)$$

$$Z^0 \rightarrow 4 \text{ jets} \quad (1.2)$$

We have in mind experiments at highest PETRA or PEP energies and at LEP energies, where Z^0 -bosons should be produced abundantly. Experimental evidence for the existence of 4-jet events at PETRA energies has already been presented [14].

In QCD two types of parton final states contribute

¹ permanent address

to the reactions (1.1) and (1.2), quark–gluon states and pure quark states:

$$\gamma^*, Z^0 \rightarrow q + \bar{q} + G + G \quad (1.3)$$

$$\gamma^*, Z^0 \rightarrow q + \bar{q} + q + \bar{q} \quad (1.4)$$

At present it seems difficult to identify quark and gluon jets event by event. Therefore, we looked for a test of the triple gluon vertex which does not require jet identification. We assume, however, that experimentalists are able to reconstruct the original parton momenta from the observed hadron distributions using some cluster algorithm [15]. Therefore, we present distributions calculated at the parton level and ignore hadronization.

Our work is organized as follows. In Sect. 2 we explain the principle of our test using simple helicity and angular momentum arguments. We also give analytic expressions for a limiting case. In Sect. 3 we present the complete results of our calculation for $e^+ e^-$ -annihilation via a virtual photon in numerical form. To test the sensitivity of our correlations to the dynamics of QCD, we compare the QCD prediction to the prediction of an abelian gluon model “QED” as introduced in [16] and to a model where four jets are generated with a phase space distribution (PS-model). In Sect. 4 we discuss the decay of the Z^0 -boson into four jets. In Sect. 5 we present our conclusions.

Throughout this paper we will work to leading order in the strong coupling constant α_s and set quark masses to zero. At LEP energies this latter approximation should be reasonable for all quarks except for the top quark (if it exists). Events involving top quark production and fragmentation will presumably be identifiable by their topology.

2) The Principle of Our Test

Consider electron–positron annihilation into hadrons via a virtual photon

$$e^+ + e^- \rightarrow \gamma^* \rightarrow \text{hadrons} \quad (2.1)$$

The analysis of the 3-jet events [3, 7] tells us that quarks can emit a vector particle, a gluon, in a bremsstrahlung type process (Fig. 1). Taking this for granted, it is clear that we expect the occurrence of 4-jet events. We can, for instance, make the gluon in Fig. 1 virtual and let it decay into a quark–antiquark pair (Fig. 2a), or we can emit two gluons from the original quark line (Fig. 2b). These processes involve only the same vertex as the 3-jet events (Fig. 1). In QCD a new vertex arises where a virtual gluon splits into two gluons (Fig. 2c). The aim is to establish the existence of this latter type of diagram.

For a general 4-jet event we label the momenta as follows, working in the c.m. system.

$$\begin{aligned} e^-(k) + e^+(k') &\rightarrow \text{jet}(p_1) + \text{jet}(p_2) \\ &+ \text{jet}(p_3) + \text{jet}(p_4) \end{aligned} \quad (2.2)$$

$$s = (k + k')^2 = (p_1 + p_2 + p_3 + p_4)^2$$

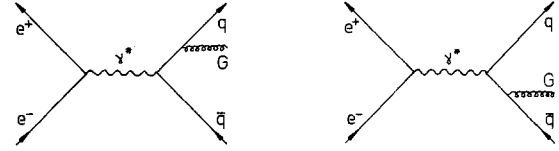


Fig. 1. Lowest order diagrams for the reaction $e^+ e^- \rightarrow \gamma^* \rightarrow 3$ jets in QCD

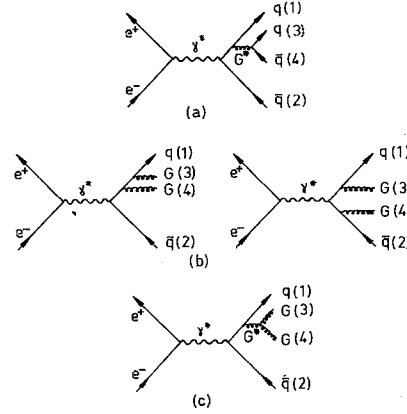


Fig. 2a–c. Examples for the three types of diagrams in QCD leading to four jets in $e^+ e^-$ -annihilation. Splitting of a virtual gluon G^* into a quark–antiquark pair **a**. Emission of two gluons from a quark line **b**. Splitting of a virtual gluon G^* into two gluons **c**. The complete list of diagrams is shown for instance in [17]. The meaning of the numbers (1)–(4) is explained in the text

$$\begin{aligned} |\mathbf{p}_i| &= E_i \quad (i = 1, 2, 3, 4) \\ E_1 &\geq E_2 \geq E_3 \geq E_4 \end{aligned} \quad (2.3)$$

We will always refer to the most energetic jet as jet 1, to the second most energetic as jet 2, and so on.

To find a clear signal for the triple gluon vertex, we will consider very simple 4-jet events consisting of two back to back jets of high energy and two back to back jets of much lower energy.

$$\begin{aligned} \mathbf{p}_1 + \mathbf{p}_2 &= 0 \\ \mathbf{p}_3 + \mathbf{p}_4 &= 0 \\ E_1 = E_2 &\gg E_3 = E_4 \end{aligned} \quad (2.4)$$

We show this in Fig. 3 where we also indicate the relevant angles which we will use.

$$\begin{aligned} \cos \vartheta_1 &= \frac{\mathbf{k} \cdot \mathbf{p}_1}{|\mathbf{k}| |\mathbf{p}_1|} \\ \cos \vartheta_{13} &= \frac{\mathbf{p}_1 \cdot \mathbf{p}_3}{|\mathbf{p}_1| |\mathbf{p}_3|} \end{aligned} \quad (2.5)$$

Since we assume unidentified jets, the kinematic angular range is given by

$$\begin{aligned} 0 &\leq \vartheta_1 \leq \pi/2 \\ 0 &\leq \vartheta_{13} \leq \pi/2 \end{aligned} \quad (2.6)$$

To avoid infrared and collinear singularities, we have

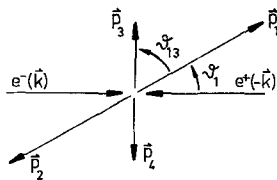


Fig. 3. A four-jet event consisting of two pairs of back to back jets of high and low energy, respectively

to stay away from $\vartheta_{13} = 0$ and $E_3 = 0$. Details on our cuts will be given in the next section.

We claim that the distribution in the angle ϑ_{13} which is the angle between the axis of the high energy jets 1 and 2 and the low energy jets 3 and 4 is very sensitive to the presence of the triple gluon coupling. To make the argument simple, let us, in this section, make an expansion in powers of E_3/E_1 and keep only the leading term. The first observation is that in this leading order the high energy jets 1 and 2 are always formed by the originally produced $q\bar{q}$ -pair. This is understandable since the multi-jet production is a bremsstrahlung type process. The low energy jets (3 and 4) must then come from the secondarily produced quark-antiquark pair or from the two gluons. In the diagrams of Fig. 2 we can, therefore, identify the jets 1–4 with quarks and gluons as indicated by the numbers (1)–(4). Of course, the permutations $1 \leftrightarrow 2$, and $3 \leftrightarrow 4$ give equally leading configurations.

Let us concentrate next on the diagrams of the type shown in Figs. 2a and 2c, where we choose to work in the Landau gauge. For our 4-jet configurations the virtual gluon G^* decays at rest in the overall c.m. system, in Fig. 2a into two spin 1/2 particles, in Fig. 2c into two massless vector particles. Our idea is to look for a distribution showing clearly the different helicities of the decay products of the virtual gluon G^* .

What can we say on the spin state of our virtual gluon? We find the virtual gluon G^* to have in leading order in E_3/E_1 always helicity 0 with respect to the direction of the high energy jets 1 and 2. If the jets 1 and 2 are produced in the beam direction, helicity 0 for the gluon G^* is even dictated by angular momentum conservation and γ_5 -invariance. To see this we note that γ_5 -invariance in massless QED requires the virtual photon γ^* to have angular momentum $J_z = \pm 1$ where we take the direction of the electron momentum as positive z -axis (Fig. 4).

In massless QCD, γ_5 -invariance holds as well. Therefore the helicities of the high energy quark-antiquark pair (1 and 2 in Fig. 2) must be opposite and this $q\bar{q}$ -pair carries ± 1 unit of angular momentum with respect to its direction of flight. If the jets 1 and 2 are produced in the beam direction, angular momentum conservation requires the virtual gluon G^* in the diagrams Fig. 2a and 2c to have $J_z = 0$ or ± 2 . Since $J_z = \pm 2$ is excluded for a vector particle, the gluon G^* must have $J_z = 0$ in this case (Fig. 4).

For other directions of the jets 1 and 2 helicity zero

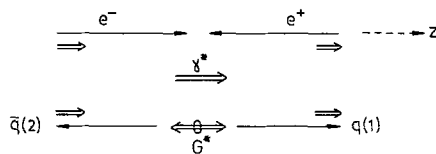


Fig. 4. An allowed helicity configuration in the reaction $e^+ e^- \rightarrow \gamma^* \rightarrow q(1) + \bar{q}(2) + G^*$ with \mathbf{p}_1 and \mathbf{p}_2 in the beam direction. We indicate helicities and angular momenta by double arrows. For helicity zero we use the symbol \leftrightarrow

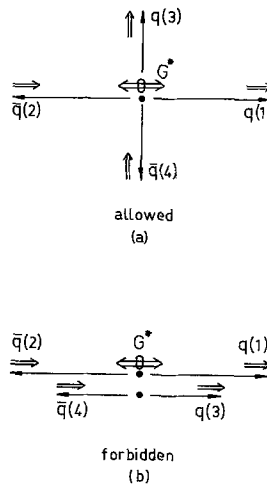


Fig. 5a and b. Allowed a and forbidden b four-jet configurations for the final state $q(1)\bar{q}(2)q(3)\bar{q}(4)$ from the diagrams of type Fig. 2a

for the gluon G^* holds only in leading order in E_3/E_1 . This can be understood since for a gluon G^* with energy $2E_3 \ll E_1$ the virtual quark in Figs. 2a and 2c is essentially on shell. This implies that only the component of the virtual photon γ^* with angular momentum ± 1 in the direction of jets 1 and 2 couples in leading order in E_3/E_1 . Now the argument continues as before. Let us also note that in elementary quantum mechanics we learn that a vector particle like our gluon G^* with helicity zero in one direction has only helicity components ± 1 in any orthogonal direction.

Next we turn to the decay of the virtual gluon G^* which in Fig. 2a goes to a massless $q\bar{q}$ -pair forming jets 3 and 4. The same γ_5 -invariance argument as before, but now applied to $G^* \rightarrow q(3) + \bar{q}(4)$, says that this *cannot* happen for jets 3 and 4 in the direction of the jets 1 and 2, but is allowed for jets 3 and 4 orthogonal to jets 1 and 2 (Fig. 5). If the virtual gluon G^* decays into two real gluons which must have helicity ± 1 , the situation is just the reverse! The two gluons can only give angular momentum 0 and ± 2 with respect to their direction of flight. Therefore, they can easily be emitted in the direction of jets 1 and 2 (Fig. 6a). But with respect to any direction orthogonal to jets 1 and 2 the virtual gluon G^* has only angular momentum components ± 1 and thus cannot emit 2 gluons in this direction (Fig. 6b). To summarize, we expect the following distributions in the angle ϑ_{13}

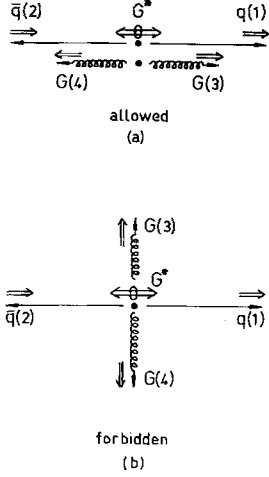


Fig. 6a and b. Allowed **a** and forbidden **b** four-jet configurations for the final state $q(1)\bar{q}(2)G(3)G(4)$ from the diagrams of type Fig. 2c involving the triple gluon vertex

(Fig. 3) from the diagrams Figs. 2a and 2c.

$$\frac{d\sigma}{d\cos\vartheta_{13}} \propto 1 - \cos^2\vartheta_{13} \quad \text{for the final state } q\bar{q}q\bar{q} \quad \text{(diagrams of type Fig. 2a)} \quad (2.7)$$

$$\frac{d\sigma}{d\cos\vartheta_{13}} \propto \cos^2\vartheta_{13} \quad \text{for the final state } q\bar{q}GG \quad \text{from diagrams of type Fig. 2c} \quad (2.8)$$

We would, therefore, expect the distribution in the angle ϑ_{13} to tell us clearly if the produced jets 3 and 4 carry predominantly helicity $\pm 1/2$ or ± 1 .

Of course, in reality life is more complicated due to the double bremsstrahlung type diagrams Fig. 2b which interfere with the diagrams containing the triple gluon vertex (Fig. 2c). But it is easy to calculate analytically the distributions for our 4-jet configurations in leading order in E_3/E_1 . We find for QCD with f massless quark flavors the following result:

$$\begin{aligned} \frac{1}{\sigma_0} d\sigma(e^+ e^- \rightarrow \text{jet}(p_1) + \text{jet}(p_2) + \text{jet}(p_3) + \text{jet}(p_4)) \\ = dx_1 dx_2 d\Omega_1 d\Omega_2 d\Omega_3 (1 + \cos^2\vartheta_1) \\ \cdot 3 \frac{\alpha_s^2}{(2\pi)^5} \left(\frac{E_1}{E_3}\right)^4 \frac{1}{\sin^4\vartheta_{13}} F_{\text{QCD}}^{(0)}(\vartheta_{13}) \left\{ 1 + O\left(\frac{E_1}{E_3}\right) \right\} \end{aligned} \quad (2.9)$$

where

$$x_i = \frac{2E_i}{\sqrt{s}}; \quad i = 1, 2 \quad (2.10)$$

$$0 \leq x_i \leq 1 \quad (2.11)$$

$$\sigma_0 = \frac{4\pi\alpha^2}{s} \sum_{j=1}^f Q_j^2 \quad (2.11)$$

$$F_{\text{QCD}}^{(0)}(\vartheta_{13}) = \frac{28}{9} + \frac{1}{2} \cos^2\vartheta_{13} \cdot (13 - 6\cos^2\vartheta_{13} + \cos^4\vartheta_{13}) + \frac{f}{6} (1 - \cos^2\vartheta_{13})^3 \quad (2.12)$$

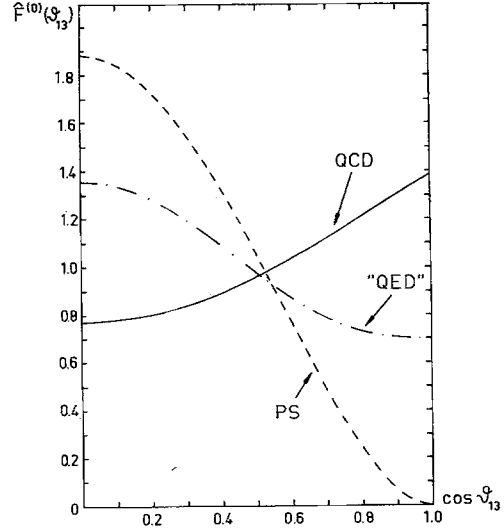


Fig. 7. The normalized functions $\hat{F}^{(0)}(\vartheta_{13})$ for QCD (2.13) and for the abelian gluon model "QED" (2.17) taking always five massless quark flavors ($f = 5$). The curve for the phase space model (PS) (2.19) is also shown

Here $\Omega_{1,2,3}$ are the solid angles of the jet momenta $\mathbf{p}_1, \mathbf{p}_2, \mathbf{p}_3, \mathbf{Q}_j$ is the charge of the j 'th quark flavor and σ_0 is the zero order cross section for $e^+ e^-$ -annihilation into hadrons. The term in $F_{\text{QCD}}^{(0)}(\vartheta_{13})$ proportional to the number of quark flavors f is the contribution from the $q\bar{q}q\bar{q}$ final states, the remaining terms come from the $q\bar{q}GG$ final states. The contribution from the $q\bar{q}q\bar{q}$ final states (diagrams of type Fig. 2a) shows a $(1 - \cos^2\vartheta_{13})^3$ behaviour consistent with (2.7) taking into account the explicit factor $1/\sin^4\vartheta_{13}$ in (2.9). This latter factor is typical for the double bremsstrahlung diagrams (Fig. 2b) which are also responsible for the more complicated form of the contribution from $q\bar{q}GG$ final states in (2.12) compared to the naive expectation (2.8). But the fact that the diagrams with the triple gluon coupling (Fig. 2c) cannot contribute when the high and low energy jets are emitted at right angles to each other leads to a pronounced minimum of the function $F_{\text{QCD}}^{(0)}(\vartheta_{13})$ for any realistic number of flavors f . This we show in Fig. 7 where we took $f = 5$ and plotted the normalized function

$$\hat{F}_{\text{QCD}}^{(0)}(\vartheta_{13}) = \frac{1}{N_{\text{QCD}}^{(0)}} F_{\text{QCD}}^{(0)}(\vartheta_{13}) \quad (2.13)$$

$$\begin{aligned} N_{\text{QCD}}^{(0)} &= \int_0^1 d(\cos\vartheta_{13}) F_{\text{QCD}}^{(0)}(\vartheta_{13}) \\ &= \frac{1496}{315} + \frac{8}{105} f \\ &\simeq 4.75 + 0.08 \cdot f \end{aligned} \quad (2.14)$$

To check the sensitivity of our correlation to the dynamics of QCD we give now the cross section for our 4-jet events calculated in the abelian gluon model "QED" as introduced in [16]. In this model the gluon carries no color and has no selfcoupling. Therefore

only diagrams of the type shown in Figs. 2a and 2b survive. The resulting cross section has the same structure as shown in (2.9) with the following replacements

$$\alpha_s \rightarrow \alpha_A = \frac{4}{3}\alpha_s \quad (2.15)$$

$$F_{\text{QCD}}^{(0)}(\vartheta_{13}) \rightarrow F_{\text{QED}}^{(0)}(\vartheta_{13}) = 4 + \frac{3}{4}f(1 - \cos^2 \vartheta_{13})^3 \quad (2.16)$$

Here α_A is the coupling strength of the abelian gluon model normalized to give the same rate of three-jet events as QCD. In $F_{\text{QED}}^{(0)}$ (2.16) the $q\bar{q}GG$ final states (the diagrams of Fig. 2b) give a constant contribution, the $q\bar{q}q\bar{q}$ final states (the diagrams of Fig. 2a) give the term proportional to f with a behaviour as expected from (2.7). In Fig. 7 we show the resulting normalized function $\hat{F}_{\text{QED}}^{(0)}(\vartheta_{13})$ defined in analogy to (2.13).

$$\hat{F}_{\text{QED}}^{(0)}(\vartheta_{13}) = \frac{1}{N_{\text{QED}}^{(0)}} F_{\text{QED}}^{(0)}(\vartheta_{13}) \quad (2.17)$$

$$\begin{aligned} N_{\text{QED}}^{(0)} &= \int_0^1 d(\cos \vartheta_{13}) F_{\text{QED}}^{(0)}(\vartheta_{13}) \\ &= 4 + \frac{12}{35}f \end{aligned} \quad (2.18)$$

Finally we discuss a phase space (PS) model for 4 jets. Here the cross section should show no dependence on $\cos \vartheta_{13}$, therefore we have for the normalized function

$$\hat{F}_{\text{PS}}(\vartheta_{13}) = \frac{15}{8}(1 - \cos^2 \vartheta_{13})^2 \quad (2.19)$$

This is also shown in Fig. 7.

As we see from Fig. 7, our correlation shows a clear difference between the QCD case and the ‘‘QED’’ and phase space model. As discussed at the beginning of this section (cf. (2.7), (2.8)), the rising curve for QCD can be interpreted as *direct* evidence for a virtual gluon decaying to two ‘‘real’’ gluons. We note that we must stay away from $\cos \vartheta_{13} = 1$ where perturbation theory breaks down due to collinear divergences. But even excluding the very forward direction, the different behaviour of the QCD, ‘‘QED’’, and PS curves in Fig. 7 should be clearly observable. For the 4-jet configuration Fig. 3 of two pairs of exactly back to back jets we have also calculated the next term in the expansion of the cross section in powers of E_3/E_1 . The result is simple if we integrate over all orientations of the final state relative to the direction of the $e^+ e^-$ beams. We obtain

$$\begin{aligned} \frac{1}{\sigma_0} d\sigma(e^+ e^- \rightarrow 4 \text{ jets}) &= dx_1 dx_2 d\Omega_2 d(\cos \vartheta_{13}) \\ &\cdot 4 \frac{\alpha_s^2}{(2\pi)^3} \left(\frac{E_1}{E_3}\right)^4 \frac{1}{\sin^4 \vartheta_{13}} \\ &\cdot \left\{ F_{\text{QCD}}^{(0)}(\vartheta_{13}) + \frac{E_3}{E_1} F_{\text{QCD}}^{(1)}(\vartheta_{13}) + O\left(\alpha_s \left(\frac{E_3}{E_1}\right)^2\right) \right\} \end{aligned} \quad (2.20)$$

where $F_{\text{QCD}}^{(0)}(\vartheta_{13})$ is as in (2.12) and

$$\begin{aligned} F_{\text{QCD}}^{(1)}(\vartheta_{13}) &= \frac{122}{9} + \frac{1}{18}\cos^2 \vartheta_{13} \\ &\cdot (161 - 12\cos^2 \vartheta_{13} - 9\cos^4 \vartheta_{13}) \end{aligned}$$

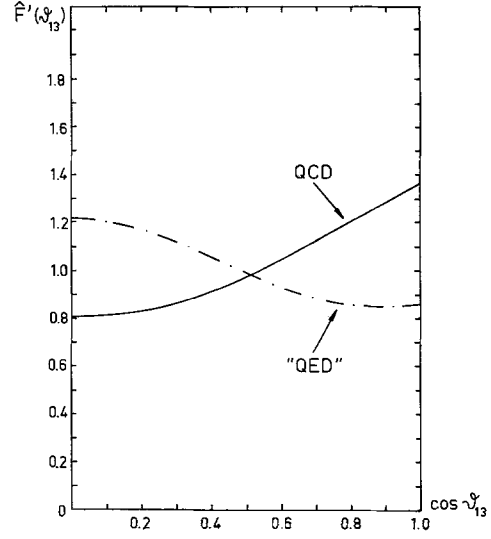


Fig. 8. The normalized functions $\hat{F}'(\vartheta_{13})$ (2.23) corresponding to the next to leading order result in E_3/E_1 for $E_3/E_1 = 1/4$. The curves are shown for QCD and the ‘‘QED’’ model

$$+ \left[\left(\frac{5}{24} \cdot f \cdot \cos^2 \vartheta_{13} - \frac{1}{9} \right) (1 - \cos^2 \vartheta_{13})^2 \right] \quad (2.21)$$

For the abelian model ‘‘QED’’ we have again to make the replacements (2.15) and (2.16) and in addition

$$\begin{aligned} F_{\text{QCD}}^{(1)}(\vartheta_{13}) \rightarrow F_{\text{QED}}^{(1)}(\vartheta_{13}) &= \frac{61}{8} + \frac{1}{8}\cos^2 \vartheta_{13} \\ &\cdot (38 - 3\cos^2 \vartheta_{13}) \\ &+ \left[\left(\frac{15}{16} \cdot f \cdot \cos^2 \vartheta_{13} + \frac{1}{2} \right) (1 - \cos^2 \vartheta_{13})^2 \right] \end{aligned} \quad (2.22)$$

Note that the pure quark–antiquark final states contribute the terms in square brackets in (2.21) and (2.22) which are no longer simply proportional to the number of flavors f .

In Fig. 8 we show the normalized distributions in $\cos \vartheta_{13}$ for $E_3/E_1 = 1/4$ for QCD and ‘‘QED’’

$$\begin{aligned} \hat{F}'(\vartheta_{13}) &= \frac{1}{N'} (F^{(0)}(\vartheta_{13}) + \frac{1}{4}F^{(1)}(\vartheta_{13})) \\ N' &= \int_0^1 d(\cos \vartheta_{13}) (F^{(0)}(\vartheta_{13}) + \frac{1}{4}F^{(1)}(\vartheta_{13})) \end{aligned} \quad (2.23)$$

Comparing with Fig. 7 we see that inclusion of the next order in E_3/E_1 makes little difference.

In this section we have only dealt with the general idea of our test and the results to leading and next to leading order in E_3/E_1 . In the next section we present the result of the complete calculation for $e^+ e^-$ annihilation for a realistic choice of cuts in energies and angles.

3) Results for the Reaction $e^+ e^- \rightarrow \gamma^* \rightarrow 4$ Jets

For a comparison with real data the results for two pairs of exactly back to back jets (Fig. 3) presented in section 2 are not sufficient. We have to allow configura-

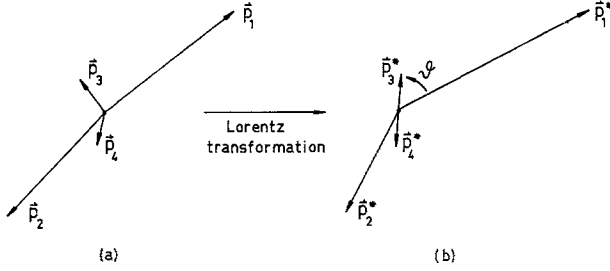


Fig. 9. **a** A four-jet event consisting of two pairs of almost back to back jets of high energy and low energy in the c.m. system. **b** The same event in the rest system of the low energy jets. The angle ϑ (3.7) is indicated

tions of the four jets where the jet momenta are not exactly back to back.

To define a suitable four-jet sample we first label the jets according to energy (2.3). Next we select four-jet events consisting of two almost back to back jets of high energy and two almost back to back jets of lower energy by requiring

$$\frac{E_3}{E_2} < \varepsilon = \frac{1}{3} \quad (3.1)$$

With a small value of ε we select events where jets 1 and 2 are almost back to back, since clearly for $\varepsilon \rightarrow 0$ we approach a two-jet event. To avoid, however, the two- and three-jet region where the infrared divergences show up, we require that the invariant mass of the two low energy jets exceeds a given value M_c

$$(p_3 + p_4)^2 \geq M_c^2 = 0.04 \cdot s \quad (3.2)$$

For $\sqrt{s} = 40$ GeV this gives $M_c = 8$ GeV. Finally we have to avoid singular configurations due to collinear jet momenta. This we do by requiring the angles between any two jets to be bigger than some minimal angle ϑ_{\min} which we choose as 25° .

$$\cos \vartheta_{ij} = \frac{\mathbf{p}_i \cdot \mathbf{p}_j}{|\mathbf{p}_i| |\mathbf{p}_j|} \quad (i, j = 1, \dots, 4) \quad (3.3)$$

$$\vartheta_{ij} > \vartheta_{\min} = 25^\circ \quad (3.4)$$

This is a limit below which an experimental resolution of two jets seems impossible anyhow. A typical event surviving our cuts is shown in Fig. 9a in the c.m. system.

We have now various possibilities to define an angle ϑ which reduces to ϑ_{13} in the ideal back to back configuration (Fig. 3). We choose the following procedure. We perform for every accepted event a Lorentz transformation Λ into the rest system of the two low energy jets

$$p_i^{*\mu} = \Lambda_i^\nu p_i^\nu \quad (i = 1, \dots, 4) \quad (3.5)$$

This is shown in Fig. 9b. We define

$$\mathbf{p}^* = \begin{cases} \mathbf{p}_1^* & \text{if } E_1^* \geq E_2^* \\ \mathbf{p}_2^* & \text{if } E_2^* \geq E_1^* \end{cases} \quad (3.6)$$

$$E^* = |\mathbf{p}^*|$$

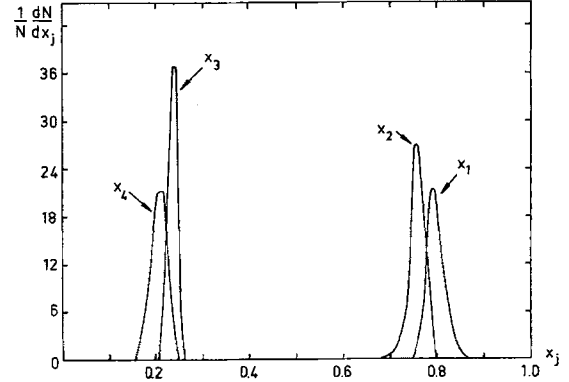


Fig. 10. The normalized distributions of the scaled energies (3.12) for our four-jet sample defined by (3.1), (3.2), and (3.4)

$$\cos \vartheta = \max \left\{ \frac{\mathbf{p}_3^* \cdot \mathbf{p}^*}{|\mathbf{p}_3^*| |\mathbf{p}^*|}, \frac{\mathbf{p}_4^* \cdot \mathbf{p}^*}{|\mathbf{p}_4^*| |\mathbf{p}^*|} \right\} \quad (3.7)$$

The kinematical angular range for ϑ is given by

$$0 \leq \vartheta \leq \pi/2 \quad (3.8)$$

Note that for ideal configurations (Fig. 3) we obviously have

$$\vartheta = \vartheta_{13} \quad (3.9)$$

We have now calculated the cross section and the distributions for the reaction

$$e^+ e^- \rightarrow \gamma^* \rightarrow \text{four jets} \quad (3.10)$$

in leading order QCD where the four jets satisfy the requirements (3.1), (3.2), and (3.4). The analytic expressions for the unintegrated four-jet cross sections for the contributing parton processes

$$\begin{aligned} e^+ e^- \rightarrow \gamma^* \rightarrow q\bar{q}GG \\ e^+ e^- \rightarrow \gamma^* \rightarrow q\bar{q}q\bar{q} \end{aligned} \quad (3.11)$$

are known [13, 16, 18, 19]. Integrations over phase space were done using the Monte Carlo program FOWL [20]. In Fig. 10 we show for our four-jet sample the normalized distributions of the scaled energies

$$x_j = \frac{2E_j}{\sqrt{s}} \quad (j = 1, \dots, 4) \quad (3.12)$$

The normalized distributions of the angles ϑ_{12} and ϑ_{34} between the two high energy jets 1 and 2 and the two low energy jets 3 and 4 are shown in Fig. 11. We see that indeed our cuts select a sample of four-jet events coming close to the ideal configuration of Fig. 3.

Motivated by our discussion in Sect. 2 we have calculated a distribution function $F(\vartheta)$ defined as the cross section weighted with a convenient factor and integrated over the accepted phase space region at fixed ϑ .

$$F(\vartheta) = \frac{1}{\sigma_0} \sin^4 \vartheta \int_{\text{accepted phase space}} dE^* dE_3^*$$

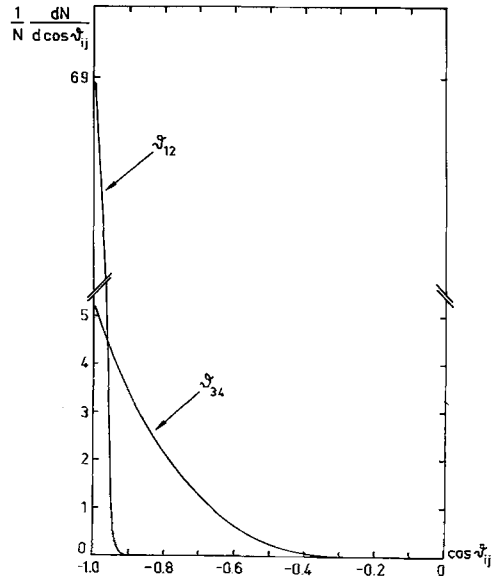


Fig. 11. The normalized distributions in the angle ϑ_{12} between the two high energy jets and in the angle ϑ_{34} between the two low energy jets (cf. (3.3))

$$\left(\frac{E_3^*}{E^*}\right)^4 \frac{\partial^3 \sigma(e^+ e^- \rightarrow 4 \text{ jets})}{\partial \cos \vartheta \partial E_3^* \partial E_4^*} \quad (3.13)$$

where σ_0 is the zero order cross section (2.11). The corresponding normalized function

$$\hat{F}(\vartheta) = \frac{1}{N} F(\vartheta) \quad (3.14)$$

$$N = \int_0^1 d(\cos \vartheta) F(\vartheta) \quad (3.15)$$

is shown in Fig. 12. The normalization factor N is given in Table 1.

The function $F(\vartheta)$ (3.13) is apart from multiplicative factors the generalization of $F_{\text{QCD}}^{(0)}(\vartheta_{13})$ (2.12). We can, therefore, directly compare the normalized function $\hat{F}(\vartheta)$ (3.14) shown as QCD curve in Fig. 12, with the corresponding curve for the ideal jet configuration in leading order in E_3/E_1 shown in Fig. 7. We see that the minimum at $\cos \vartheta = 0$ for the QCD curve is still clearly visible in the realistic jet sample (Fig. 12). The sharp drop of the curves in Fig. 12 for $\cos \vartheta \rightarrow 1$ is of course due to our cut (3.4) which avoids collinear configurations.

In Fig. 12 we also show the normalized distribution functions $\hat{F}(\vartheta)$ (3.14) for the abelian gluon model "QED" and for the phase space model PS. The normalization factor N for "QED" is given in Table 1 where we have used again the relation (2.15). Both "QED" and the PS-model show an almost flat behaviour for

$$0 \leq \cos \vartheta < 0.60 \quad (3.16)$$

We think, therefore, that the minimum of the QCD-

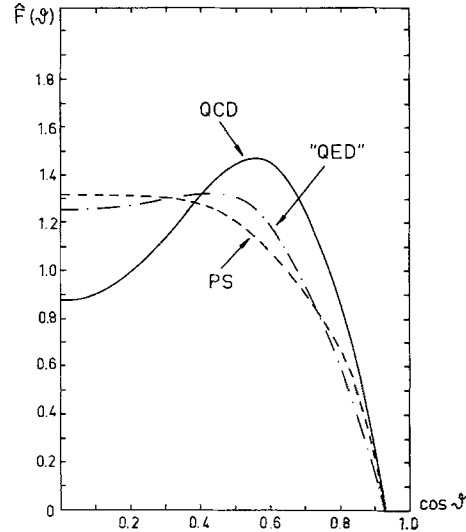


Fig. 12. The normalized distribution function $\hat{F}(\vartheta)$ (3.14) for QCD, "QED", and the phase space model (PS). The QCD and "QED" curves are for five massless quark flavors ($f = 5$)

Table 1. The normalization factor N (3.15) and the fraction of the total hadronic cross section giving four jets which satisfy our criteria (3.1), (3.2), and (3.4). The results are given for QCD and the abelian model "QED". The errors are due to the Monte Carlo calculation

	N	$\frac{1}{\sigma_0} \sigma(e^+ e^- \rightarrow \gamma^* \rightarrow 4 \text{ jets})$
QCD	$(4.48 \pm 0.04) \cdot 10^{-5} \cdot \alpha_s^2$	$(0.0454 \pm 0.0004) \cdot \alpha_s^2$
"QED"	$(6.26 \pm 0.06) \cdot 10^{-5} \cdot \alpha_s^2$	$(0.0531 \pm 0.0005) \cdot \alpha_s^2$

curve for $\cos \vartheta = 0$ can be interpreted as clear signal for the triple gluon vertex.

Let us note that our normalized distributions (Fig. 12) are independent of the c.m. energy \sqrt{s} . This is easy to see as we are considering QCD and the "QED" model at the tree graph level and for massless quarks. Since also our cuts (3.1), (3.2), and (3.4) are scale-invariant the only energy dependence enters through α_s in the normalization factor N of Table 1. In the phase space model (PS) for massless jets there is no energy dependence anyway.

We give in Table 1 also the total cross section for our accepted four-jet sample normalized to the zero order cross section (2.11). Taking for the QCD case a value of $\alpha_s = 0.15$ which is a typical value obtained for $\sqrt{s} \simeq 33$ GeV from three-jet analyses (cf. the reviews in [21]) and four-jet analyses [14] we find that our accepted four-jet sample corresponds to roughly 0.1% of the total hadronic cross section. Since this fraction is quite small for present statistics, it might be easier to consider integrated quantities. We can, for instance,

Table 2. Ratio ρ as defined in (3.17) for QCD, the abelian model (“QED”), and the phase space model (PS)

	ρ
QCD	0.146 ± 0.008
“QED”	-0.019 ± 0.008
PS	-0.074 ± 0.004

make two bins in $\cos \vartheta$ and define

$$\rho = \frac{\int_{0.35}^{0.70} d(\cos \vartheta) F(\vartheta) - \int_0^{0.35} d(\cos \vartheta) F(\vartheta)}{\int_0^{0.70} d(\cos \vartheta) F(\vartheta)} \quad (3.17)$$

The results for ρ are given in Table 2 and also show quite clearly the difference between QCD, “QED” and the phase space model (PS).

4) Results for the Decay $Z^0 \rightarrow$ Four Jets

With accelerators reaching c.m. energies of ~ 100 GeV the production and decay of the Z^0 -boson, if it exists, should become observable. In the standard model [22] the Z^0 -boson is expected to decay with a branching ratio of $\sim 70\%$ to hadrons. These hadronic final states should show jet patterns similar to the final states in $e^+ e^-$ -annihilation through a virtual photon. The high mass of the Z^0 and its expected high production rates at storage rings like LEP should, therefore, make Z^0 -decay the ideal reaction for testing QCD predictions for jets.

In this section we will, therefore, discuss the decay $Z^0 \rightarrow$ four hadron jets

with the four jets satisfying the same criteria as in Sects. 2 or 3, respectively. We will find that the normalized distributions for the reaction (4.1) are nearly identical to the distributions for $e^+ e^-$ -annihilation through a virtual photon γ^* .

To give the details we consider the standard model of electroweak interactions [22] where the Z^0 -boson couples to leptons and quarks in the following manner

$$\mathcal{L}' = \frac{e}{2 \sin \vartheta_w \cos \vartheta_w} Z^\mu J_\mu^{NC} \quad (4.2)$$

$$J_\mu^{NC} = \sum_j (g_V^j V_\mu^j - g_A^j A_\mu^j)$$

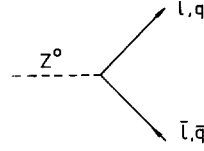
$$V_\mu^j = \bar{\Psi}_j \gamma_\mu \Psi_j; A_\mu^j = \bar{\Psi}_j \gamma_\mu \gamma_5 \Psi_j$$

where e is the positron charge and the sum runs over all fermion species. For the weak mixing angle ϑ_w we use $\sin^2 \vartheta_w = 0.23$

consistent with present experiments [23]. The weak

Table 3. The weak coupling constants g_V, g_A of (4.2) for leptons and quarks in the standard model

fermions	g_V	g_A
ν_e, ν_μ, ν_τ	$\frac{1}{2}$	$\frac{1}{2}$
e, μ, τ	$-\frac{1}{2} + 2 \sin^2 \vartheta_w$	$-\frac{1}{2}$
u, c, t	$\frac{1}{2} - \frac{4}{3} \sin^2 \vartheta_w$	$\frac{1}{2}$
d, s, b	$-\frac{1}{2} + \frac{2}{3} \sin^2 \vartheta_w$	$-\frac{1}{2}$

**Fig. 13.** Diagram for the decay of the Z^0 into a fermion–antifermion pair in lowest order, where l stands for lepton, q for quark

coupling constants for leptons and quarks are listed in Table 3.

In *lowest order* of electroweak and strong interactions the Z^0 mass is given by

$$m_Z^2 = \frac{\pi\alpha}{\sqrt{2} G \sin^2 \vartheta_w \cos^2 \vartheta_w} \simeq (89 \text{ GeV})^2 \quad (4.4)$$

where α is the fine structure constant and G is Fermi’s constant. The Z^0 -decay goes to a lepton–antilepton or quark–antiquark pair giving two hadron jets (Fig. 13). The decay rate for any fermion species j of mass m_j is given by

$$\Gamma(Z^0 \rightarrow j + \bar{j}) = 2N_c^j \left(1 - \frac{4m_j^2}{m_Z^2}\right)^{1/2} \cdot \left\{ (g_V^j)^2 \left(1 + \frac{2m_j^2}{m_Z^2}\right) + (g_A^j)^2 \left(1 - \frac{4m_j^2}{m_Z^2}\right) \right\} \Gamma_\nu$$

$$\Gamma_\nu = \frac{\alpha m_Z}{24 \sin^2 \vartheta_w \cos^2 \vartheta_w} \simeq 0.15 \text{ GeV} \quad (4.5)$$

$$N_c^j = \begin{cases} 1 & \text{for leptons} \\ 3 & \text{for quarks} \end{cases}$$

where Γ_ν is the rate for the decay into one neutrino flavor in the standard model (cf. table 3).

In higher orders in the strong interactions we will have final states containing more quarks and gluons leading to multi-jet production. The four-jet final states are due to the following parton processes

$$Z^0 \rightarrow q + \bar{q} + G + G \quad (4.6)$$

$$Z^0 \rightarrow q + \bar{q} + q + \bar{q} \quad (4.7)$$

In leading order QCD the corresponding diagrams

are as in Fig. 2 with the $e^+ e^-$ line omitted, the γ^* replaced by Z^0 and the electromagnetic coupling of the quarks replaced by the neutral current coupling (4.2).

We will again neglect quark masses, i.e. we consider only decays of the Z^0 into (nearly) massless quark flavors. This should be a valid approximation for the u, d, s, c and b quark. We can then use γ_5 -invariance to make some general statements.

The amplitudes for the processes (4.6) and (4.7) will be the sum of the contributions from the vector (V) and axial vector (A) part of the neutral current (4.2). Our four-jet samples, both the ideal one considered in Sect. 2 and the realistic one considered in Sect. 3, form a parity-even set of final states. This holds also for fixed angle ϑ_{13} (2.5) or ϑ (3.7). Thus in the corresponding differential decay rates of the Z^0 there can only be VV and AA contributions, no VA interference terms.

We will now show that the diagrams of Fig. 2b and 2c (always replacing γ^* by Z^0) leading to the $q\bar{q}GG$ final state (4.6) give for massless quarks

$$VV = AA \quad (4.8)$$

To see this we introduce the chiral currents

$$J_{\mu R, L} = \frac{1}{2}(V_\mu \pm A_\mu) \quad (4.9)$$

We have schematically

$$\begin{aligned} VV &= J_R^2 + J_L^2 + 2J_R J_L \\ AA &= J_R^2 + J_L^2 - 2J_R J_L \end{aligned} \quad (4.10)$$

For the diagrams of Fig. 2b and 2c the chiral current $J_L(J_R)$ always gives a left (right) handed quark and a right (left) handed antiquark. The final states reached through J_L and J_R are thus orthogonal and the terms $J_R J_L$ in (4.10) vanish.

For the final states $q\bar{q}q\bar{q}$ (4.7) produced by the diagrams of type Fig. 2a, the argument does not work in general, even for massless quarks. A final state $q_R \bar{q}_L q_L \bar{q}_R$ where the two quarks have opposite helicities and the two antiquarks also, can be reached both through J_R and J_L . Indeed it is easy to show that $VV \neq AA$ in general. However, for our ideal four-jet configuration considered in Sect. 2 we have in *leading order* in E_3/E_1 always tagged the high energy jets 1 and 2 as the originally produced $q\bar{q}$ -pair. In this case we have the same situation for the diagrams of type Fig. 2a as for the $q\bar{q}GG$ final state, i.e. $VV = AA$.

Using these findings we can easily give the decay rate for $Z^0 \rightarrow$ four jets in the ideal back to back configuration (Fig. 3) in leading order in E_3/E_1 . We find for f massless quark flavors

$$\begin{aligned} & \frac{1}{\Gamma_0} d\Gamma(Z^0 \rightarrow \text{jet 1} + \text{jet 2} + \text{jet 3} + \text{jet 4}) \\ &= dx_1 dx_2 d\Omega_2 d(\cos \vartheta_{13}) \\ & \cdot 4 \frac{\alpha_s^2}{(2\pi)^3} \left(\frac{E_1}{E_3}\right)^4 \frac{F_{\text{QCD}}^{(0)}(\vartheta_{13})}{\sin^4 \vartheta_{13}} \left\{ 1 + O\left(\alpha_s \frac{E_3}{E_1}\right) \right\} \end{aligned} \quad (4.11)$$

where the notation is as in Sect. 2 and Γ_0 is the zero order decay rate into our f massless quark flavors (cf. (4.5))

$$\Gamma_0 = \sum_{j=1}^f 6((g_V^j)^2 + (g_A^j)^2) \Gamma_V \quad (4.12)$$

For the ‘‘QED’’ model we have, again, to make the replacements (2.15) and (2.16). The normalized distribution functions $\hat{F}^{(0)}(\vartheta_{13})$ shown in Fig. 7 represent, therefore, also our result in leading order in E_3/E_1 for Z^0 -decay. By explicit calculation we found that $VV = AA$ holds still for all our diagrams if we include the next term in the expansion in powers of E_3/E_1 . Therefore the first correction term to (4.11) can also simply be read off from the corresponding eq. (2.20) of Sect. 2.

Next we consider the rate for Z^0 -decay into four jets satisfying the criteria of Sect. 3 ((3.1), (3.2), and (3.4)). In this case we have to do a new calculation since here indeed we find $VV \neq AA$. In analogy to (3.13)–(3.15) we define

$$\begin{aligned} F_Z(\vartheta) &= \frac{1}{\Gamma_0} \sin^4 \vartheta \int_{\text{accepted phase space}} dE^* dE_3^* \left(\frac{E_3^*}{E^*}\right)^4 \\ & \frac{\partial^3 \Gamma(Z^0 \rightarrow 4\text{jets})}{\partial \cos \vartheta \partial E^* \partial E_3^*} \end{aligned} \quad (4.13)$$

$$\hat{F}_Z(\vartheta) = \frac{1}{N_Z} F_Z(\vartheta) \quad (4.14)$$

$$N_Z = \int_0^1 d(\cos \vartheta) F_Z(\vartheta) \quad (4.15)$$

It turns out that for the neutral current couplings of u, d, s, c and b quarks (Table 3) the differences between F_Z and F, \hat{F}_Z and \hat{F} , and N_Z and N are only of the order of 0.1% both for QCD and the ‘‘QED’’ model. To this accuracy the curves of figs. 10–12 and the results of Tables 1 and 2 apply, therefore, also to Z^0 -decay. In particular we find from table 2 in the QCD case the branching ratio of Z^0 -decay into our four-jet sample to be

$$\frac{\Gamma(Z^0 \rightarrow 4\text{jets})}{\Gamma(Z^0 \rightarrow \text{all})} = \frac{\Gamma_0}{\Gamma(Z^0 \rightarrow \text{all})} \cdot (0.045) \cdot \alpha_s^2 \quad (4.16)$$

The total Z^0 -decay rate depends somewhat on the top quark mass (cf. (4.5)) which certainly cannot be neglected. But taking u, d, s, c and b quarks as massless and counting their production in Γ_0 , we can estimate

$$\begin{aligned} & \frac{\Gamma_0}{\Gamma(Z^0 \rightarrow \text{all})} \simeq 0.7 \\ & \alpha_s \simeq 0.15 \\ & \frac{\Gamma(Z^0 \rightarrow 4\text{jets})}{\Gamma(Z^0 \rightarrow \text{all})} \simeq 7 \cdot 10^{-4} \end{aligned} \quad (4.17)$$

Such a branching ratio should easily be observable

with the projected event rates of $10^4 - 10^5$ Z^0 -bosons per day at LEP.

5) Conclusion

In this paper we have considered the decay of a virtual photon γ^* or the Z^0 -boson into a very simple class of four-jet events. An experimental verification of the QCD prediction for the distribution in our angle ϑ (Fig. 12) would test both the presence of the triple gluon coupling and the masslessness of the gluon, since our helicity arguments of section 2 break down for massive gluons. We can finally ask if also the very simple angular distributions (2.7) and (2.8) could be observable which would offer an even clearer signal for the triple gluon coupling. The answer is yes, if we can develop a way to observe the linear polarization of gluons in the final state. This may not be impossible since a quark-antiquark pair produced by a linearly polarized gluon might remember the direction of the color electric field vector in the same way as an electron-positron pair remembers the direction of the electric field vector of the photon. A classic application of this effect was the determination of the parity of the π^0 -meson [24]. In our case we find for the ideal configuration (Fig. 3) and in leading order in E_3/E_1 that gluons polarized perpendicular to the event plane show the simple angular distribution (2.8).

We have in this paper given distributions calculated at the parton level and relied on cluster algorithms reconstructing the original parton axes for comparison with experiments. It would also be easy to formulate our effect for Serman-Weinberg type jets [25]. This may even be preferable when considering higher order corrections in α_s . A question we may ask in connection with these higher order corrections is if terms proportional to $\ln \varepsilon$ may wreck our leading order calculation, where ε is our limit for the ratio E_3/E_2 in (3.1). We would expect this to happen for $\varepsilon \rightarrow 0$ but for our value $\varepsilon = 1/3$ there should be no problem.

Acknowledgement. We would like to thank C. Jarlskog and our colleagues in Heidelberg and Hamburg for useful discussions and comments.

References

- G. Hanson et al.: Phys. Rev. Lett. **35**, 1609 (1975)
- Ch. Berger et al.: Phys. Lett. **78B**, 176 (1978)
- R. Brandelik et al.: Phys. Lett. **86B**, 243 (1979); D.P. Barber et al.: Phys. Rev. Lett. **43**, 830 (1979); Ch. Berger et al.: Phys. Lett. **86B**, 418 (1979); W. Bartel et al.: Phys. Lett. **91B**, 142 (1980)
- H. Abramowicz et al.: Z. Phys. C—Particles and Fields **13**, 199 (1982)
- J. Drees: Review of the structure of hadrons from lepton-nucleon interactions, in Proc. 1981 International Symposium on Lepton and Photon Interactions at High Energies, W. Pfeil, ed. (Univ. Bonn, 1981)
- Ch. Berger et al.: Phys. Lett. **86B**, 399 (1979); B. Niczyporuk et al.: Z. Phys. C—Particles and Fields **9**, 1 (1981)
- R. Brandelik et al.: Phys. Lett. **97B**, 453 (1980); Ch. Berger et al.: Phys. Lett. **97B**, 459 (1980)
- T.F. Walsh, P. Zerwas: Phys. Lett. **93B**, 53 (1980)
- A. De Rujula, R. Petronzio, B. Lautrup: Nucl. Phys. **B146**, 50 (1978); K. Koller, T.F. Walsh, P.M. Zerwas: Phys. Lett. **82B**, 263 (1979); K. Koller, K.H. Streng, T.F. Walsh, P.M. Zerwas: Nucl. Phys. **B193**, 61 (1981); K. Koller, K.H. Streng, T.F. Walsh, P.M. Zerwas: Multijet decays of quarkonia: testing the three-gluon vertex. SLAC-PUB-2858 (1981) (unpublished); A.N. Kamal et al.: Phys. Rev. **D25**, 784 (1982)
- W. Furmanski, S. Pokorski: QCD tests: 3G vertex effects. In: Proceedings of the II international Symposium on Hadron Structure and Multiparticle Production. Kazimierz, Poland, 20–26 May 1979; C.E. Carlson, P. Hoyer: Nucl. Phys. **B193**, 109 (1981); M. Glück, E. Reya: Phys. Lett. **98B**, 444 (1981)
- E. Reya: Phys. Rev. Lett. **43**, 8 (1979); K. Hagiwara, K. Hikasa, N. Kai: Phys. Rev. Lett. **47**, 983 (1981); E.N. Argyres, C.S. Lam, Bing An Li: Effect of triple gluon coupling in semi-inclusive polarized scattering processes. SLAC-PUB 2720 (1981)
- K. Fabricius, G. Kramer, G. Schierholz, I. Schmitt: Phys. Rev. Lett. **45**, 867 (1980); G. Grunberg, Y.J. Ng, S.-H.H. Tye: Phys. Lett. **93B**, 281 (1980); G. Gustafson, T. Sjöstrand: Some comments on jet structure at LEP energies. University of Lund report (1981) (unpublished)
- J.G. Körner, G. Schierholz, J. Willrodt: Nucl. Phys. **B185**, 365 (1981)
- JADE Coll., W. Bartel et al.: Observation of four-jet structure in e^+e^- -annihilation at $\sqrt{s} = 33$ GeV. Report DESY 82-016 (1981) (unpublished)
- H.J. Daum, H. Meyer, J. Bürger: Z. Phys. C—Particles and Fields **8**, 167 (1981); M.C. Goddard: A general algorithm for the reconstruction of jet events in e^+e^- annihilation, Rutherford and Appleton Laboratories report, RL-81-069
- K.J.F. Gaemers, J.A.M. Vermaseren: Z. Phys. C—Particles and Fields **7**, 81 (1980)
- O. Nachtmann, A. Reiter: Z. Phys. C—Particles and Fields **14**, 47 (1982)
- A. Ali et al.: Phys. Lett. **82B**, 285 (1979); Nucl. Phys. **B167**, 454 (1980); T. Chandramohan, L. Clavelli: Phys. Lett. **94B**, 409 (1980); Nucl. Phys. **B184**, 365 (1981); R.K. Ellis, D.A. Ross, A.E. Terrano: Phys. Rev. Lett. **45**, 1226 (1980); Nucl. Phys. **B178**, 421 (1981)
- A. Reiter: QCD-Untersuchungen zur Elektron-Positron-Annihilation in 4-jets. University of Heidelberg report, HD-THEP-81-10 (1981)
- FOWL, F. James: CERN Computer Centre, Program Library, Long write-up W 505
- R. Hollebeek, R. Felst, W. Braunschweig, D. Fournier: In Proc. 1981 International Symposium on Lepton and Photon Interactions at High Energies, W. Pfeil, ed. (Univ. Bonn, 1981)
- S. Weinberg: Phys. Rev. Lett. **19**, 1264 (1967); A. Salam: In: Elementary particle theory ed. N. Svartholm, p. 367. Stockholm: Almqvist & Wiksell; S.L. Glashow, J. Iliopoulos, L. Maiani: Phys. Rev. **D2**, 1285 (1970)
- G. Geweniger: In: Proc. Int. Conf. on Neutrinos, Weak Interactions and Cosmology, Vol. 1, p. 392, A. Haatuft, C. Jarlskog, ed., Bergen (1979); J.E. Kim, P. Langacker, M. Levine, H.H. Williams: Rev. Mod. Phys. **53**, 211 (1981)
- R. Plano et al.: Phys. Rev. Lett. **3**, 525 (1959)
- G. Serman, S. Weinberg: Phys. Lett. **39**, 1436 (1977)